Inorganic Chemistry

Article

pubs.acs.org/IC

Diversity of Copper(I) Complexes Showing Thermally Activated Delayed Fluorescence: Basic Photophysical Analysis

Rafał Czerwieniec* and Hartmut Yersin*

Institut für Physikalische und Theoretische Chemie, Universität Regensburg, 93053 Regensburg, Germany

Supporting Information

ABSTRACT: A comparison of three copper(I) compounds [**1**, Cu(dppb)-(pz_2Bph_2); **2**, Cu(pop)(pz_2Bph_2); **3**, Cu(dmp)(phanephos)$^+$] that show pronounced thermally activated delayed fluorescence (TADF) at ambient temperature demonstrates a wide diversity of emission behavior. In this study, we focus on compound **1**. A computational density functional theory (DFT)/time-dependent DFT approach allows us to predict detailed photophysical properties, while experimental emission studies over a wide temperature range down to T = 1.5 K lead to better insight into the electronic structures even with respect to spin−orbit coupling efficiencies, radiative rates, and zero-field splitting of the triplet state. All three compounds, with emission quantum yields higher than ϕ_{PL} = 70%, are potentially well suited as emitters for organic light-emitting diodes (OLEDs) based on the singlet-harvesting mechanism. Interestingly, compound **1** is by far the most attractive one because of a very small energy separation between the lowest excited singlet S_1 and triplet T_1 state of $\Delta E(S_1-T_1)$ = 370 cm^{-1} (46 meV). Such a small value has not been reported so far. It is responsible for the very short decay time of τ(TADF, 300 K) = 3.3 μs. Hence, if focused on the requirements of a short TADF decay time for reduction of the saturation effects in OLEDs, copper(I) complexes are well comparable or even slightly better than the best purely organic TADF emitters.

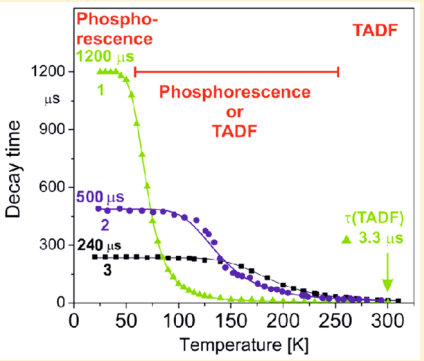

1. INTRODUCTION

Recently, research in the field of thermally activated delayed fluorescence (TADF) displayed by organo-transition-metal complexes[1−25] and organic molecules[26−35] has gained enormous interest because of the remarkable variability of the emission properties. In particular, two emitting states, an excited triplet state T_1 and an energetically slightly higher-lying singlet state S_1, are involved in the emission processes. Accordingly, the overall emission behavior depends on the individual properties of these two states, their energy separation $\Delta E(S_1-T_1)$, the related intersystem crossing (ISC) time, and the individual population rates. As a consequence, a wide range of property tuning in the sense of chemical engineering becomes possible. Thus, with a detailed understanding of the photophysical background, one may realize distinct improvements of, for example, TADF-related applications. This is particularly important for emitters used in organic light-emitting diodes (OLEDs)[12−18,20,24,28−31,33,35−37] or in light-emitting electrochemical cells.[19,38−40] In these devices, the TADF mechanism allows for the harvesting of all generated singlet and triplet excitons, whereby emission stems from the singlet state, hence representing a singlet-harvesting mechanism.[1,2,8−10,15−17] This effect is based on an alternative process different from the already well-established triplet-harvesting mechanism, which requires efficient and short-lived triplet-state emission.[1,2,41−43] Accordingly, this latter mechanism is essentially based on compounds with (high-cost) third-row transition metals that may induce high spin−orbit coupling (SOC), while the singlet-harvesting TADF-based mechanism does not depend on this requirement.

In this contribution, we focus on a mononuclear copper(I) complex, Cu(dppb)(pz_2Bph_2) (**1**), where dppb = 1,2-bis-(diphenylphosphino)benzene and pz_2Bph_2 = diphenylbis-(pyrazol-1-yl)borate (Figure 1), which shows outstanding properties with respect to an astonishingly long emission decay time at low temperature and, on the other hand, a very short decay time at ambient temperature at a high emission quantum yield of ϕ_{PL} = 70%. Moreover, this compound and its derivatives have already been applied to realize very efficient OLEDs using a vacuum deposition method.[18] However, the

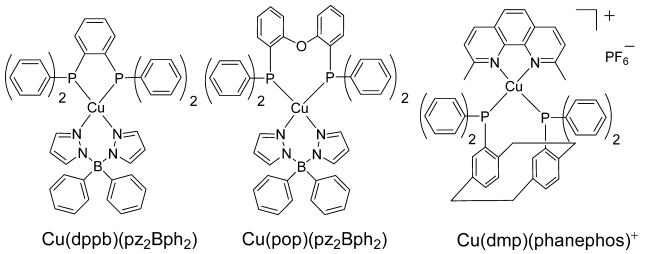

Figure 1. Chemical structures of mononuclear copper(I) complexes.

Received: December 30, 2014
Published: April 20, 2015

DOI: 10.1021/ic503072u
Inorg. Chem. 2015, 54, 4322−4327

basics of the compound's photophysical properties are not yet well understood. Therefore, a more detailed investigation will be carried out. Furthermore, the results will be briefly compared to the properties of two other mononuclear complexes, Cu(pop)(pz_2Bph_2) (**2**),[9] where pop = (oxo-2,1-phenylene)bis(diphenylphosphine), and Cu(dmp)-(phanephos)$^+$ (**3**),[10] where dmp = 2 9-dimethyl-1,10-phenanthroline and phanephos = 4,12-bis-(diphenylphosphino)[2.2]paracyclophane, which have already been studied previously (Figure 1). This comparison will demonstrate the pronounced diversity and chemical tunability of TADF-related emission properties of copper(I) compounds

2. RESULTS AND DISCUSSION

2.1. Density Functional Theory (DFT)/Time-Dependent DFT (TD-DFT) Approaches and Photophysical Interpretations. A first insight into the electronic properties of **1** can be obtained from DFT calculations by simple inspection of the frontier orbitals and corresponding energy separations. Figure 2 displays the HOMO−1, HOMO, and LUMO contour distributions of **1**. A study of these results allows us already to deduce a number of rather detailed conclusions:

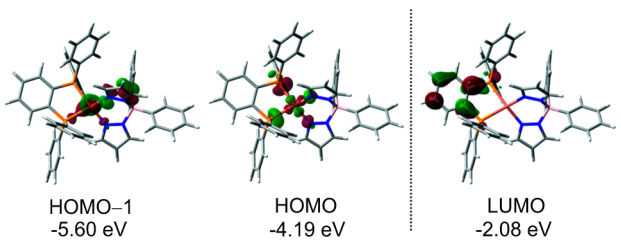

Figure 2. Frontier molecular orbitals of **1** resulting from DFT calculations for the triplet state geometry. Computational details are given in the SI.

(i) The HOMO is largely derived from a 3d atomic orbital of the copper(I) center with significant contributions from the coordinating phosphorus atoms, whereas the LUMO is mainly distributed over the *o*-phenylene ring of the dppb ligand (Figure 2). Thus, related transitions are assigned to be of metal-to-ligand charge-transfer (MLCT) character. It can be shown by TD-DFT calculations that the resulting singlet state S_1 and triplet state T_1 are to more than 90% of HOMO−LUMO character. Therefore, these states are assigned as ^{1}MLCT and ^{3}MLCT states, respectively.

(ii) The distinct spatial separation of HOMO and LUMO, as displayed in Figure 2, allows us to predict a relatively small exchange integral[44] and, thus, a small singlet−triplet energy separation $\Delta E(S_1-T_1)$. Indeed, TD-DFT calculations in the triplet-state-optimized geometry give a small value of $\Delta E(S_1-T_1) \approx 560$ cm^{-1} (Table S1 in the Supporting Information, SI).

(iii) According to the spatial separation of the involved molecular orbitals, it can be predicted that the electric dipole moment and, thus, the oscillator strength f of the transition between the electronic ground state S_0 and the lowest excited singlet state S_1 (^{1}MLCT) is relatively small. Indeed, this is supported by the TD-DFT calculations giving a value of f = 0.001 (Table S1 in the SI).

(iv) The pronounced electronic charge transfer occurring with the corresponding MLCT transitions will result in significant changes of the equilibrium positions of the atomic coordinates. Such a behavior is well established for copper(I) complexes having a pseudotetrahedral ground-state geometry but a flattened excited-state geometry. (Compare refs 45−48.)

(v) The energy separation between HOMO and HOMO−1, both involving different d orbitals, is very large (more than 1.4 eV ≈ 11300 cm^{-1}; Figure 2). As a consequence, mixing of the resulting singlet state of HOMO−1 → LUMO character to the lowest triplet state T_1 of HOMO → LUMO character by SOC (which, by symmetry, is possible[1,2,49]) is expected to be very weak. This will lead to a long emission decay time of the T_1 state and to very small values of zero-field splitting (ZFS) of this state.[1,2,49] In this context, it should be remarked that SOC between the singlet state S_1 and triplet state T_1 is forbidden because both states involve the same configuration, i.e., the same d orbital.[49−51] In fact, the T_1 decay time is as long as 1.2 ms, and the value of ZFS is less than 1 cm^{-1} (see section 2.2). In contrast, for a different compound, $Cu_2Cl_2(N\hat{}P)_2$ (with (N^P) = 2-(diphenylphosphino)-6-methylpyridine), for which the HOMO − HOMO−1 energy separation amounts only to ≈0.3 eV (2400 cm^{-1}), SOC is very effective and, indeed, a very short (radiative) emission decay time of only $\tau(T_1)$ = 42 μs and a large value of ΔE(ZFS) ≈ 15 cm^{-1} are found.[23]

Obviously, equivalent conclusions can be deduced from the TD-DFT results, in particular, with respect to the energy separation $\Delta E(S_1-T_1)$, the allowedness of the $S_0 \leftrightarrow S_1$ transition, and the energy separation between the T_1 state and the dominantly mixing state that can induce SOC, being the S_6 state (Table S1 in the SI). However, the predictions based on theoretical calculations, as given above, require an experimental verification. Indeed, this is possible and will be shown in the next section.

2.2. Phosphorescence versus TADF of 1: Detailed Characterization. 1 was synthesized according to a literature procedure.[18,52] We studied the luminescence properties in a wide temperature range from T = 1.5 to 300 K. Figure 3 displays emission spectra and decay curves of a powder sample[53] of **1** at selected temperatures. The complex shows intense green-yellow luminescence with a very high emission quantum yield of ϕ_{PL} = 70% at ambient temperature and of about 100% at T = 80 K. The spectra are broad and unstructured even at T = 1.5 K (not shown). This correlates with the predicted MLCT character of the corresponding transitions. One does not observe any significant spectral change apart from a blue shift of the emission maximum (with a temperature increase) from 548 nm (1.5 to 30 K) to 535 nm (80 to 300 K) of 13 nm (440 cm^{-1}) (Figure 3A). This blue shift is a consequence of thermal activation of the energetically higher-lying S_1 state (TADF) above $T \approx 50$ K (see also below).

On the other hand, the emission decay time exhibits drastic changes. At T = 1.5 K, one finds a strongly non-monoexponential decay, which can be well fitted by two decay components of 7.7 ms and 470 μs (Figure S1 in the SI). These are assigned to the decay times of the three individual emissions from the triplet T_1 substates I−III with $\tau_I \approx \tau_{II}$ = 7.7 ms and τ_{III} = 470 μs, respectively. The occurrence of two almost equal decay times for two triplet substates is not unusual for copper(I) complexes.[5,54] At a low temperature of T = 1.5 K, these states are not thermally equilibrated because of very slow spin−lattice relaxation (SLR) processes.[55−59] In this situation, the individual emission decay times of the three substates are much shorter than the SRL times. With a temperature increase to $T \approx 20$ K, however, these SLR processes become significantly faster (presumably according to a Raman process

DOI: 10.1021/ic503072u
Inorg. Chem. 2015, 54, 4322−4327

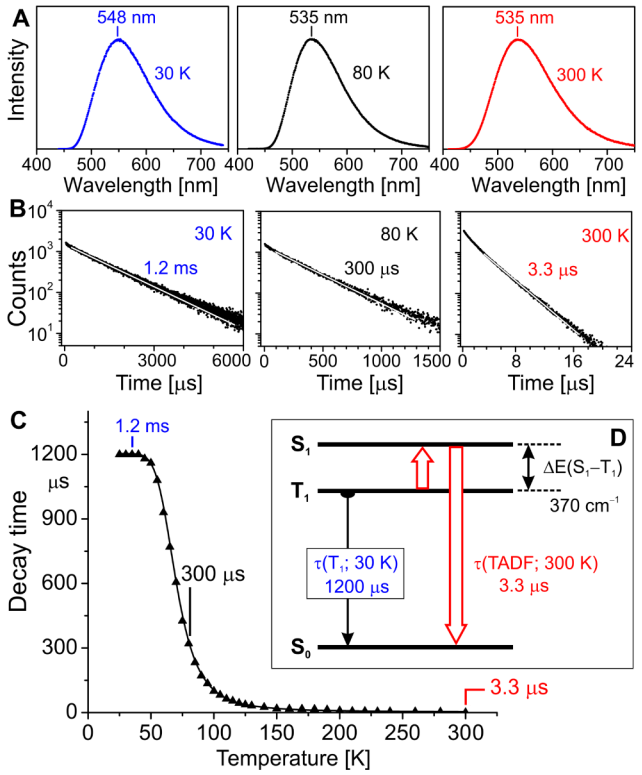

Figure 3. (A) Luminescence spectra of powder **1** recorded at 30, 80, and 300 K. (B) Emission decay profiles of **1** at 30, 80, and 300 K recorded upon pulsed excitation at λ_{exc} = 372 nm and detected at λ_{det} = 540 nm. (C) Emission decay time τ of **1** (powder) versus temperature. The solid line represents a fit of eq 1 to the experimental values. Resulting fit parameters: $\tau(S_1)$ = 180 ns and $\Delta E(S_1{-}T_1)$ = 370 cm^{-1}. (D) Energy level diagram of **1** resulting from the $\tau(T)$ analysis. Two competing emission processes are marked: phosphorescence with a decay time of $\tau(T_1)$ = 1.2 ms dominating the photophysical behavior at temperatures below 50 K and TADF determining the emission properties at higher temperatures with a measured decay time of τ(TADF, 300 K) = 3.3 μs.

of SLR[55−57]) and a fast thermalization of the three substates results, giving an average emission decay time of $\tau_{av} = 3(\tau_I^{-1} + \tau_{II}^{-1} + \tau_{III}^{-1})^{-1}$.[1,2,8,9,55,56,60] Inserting the T_1 substate decay times determined at T = 1.5 K, one obtains a value of τ_{av} = 1250 μs. Almost the same value is observed in the range of the plateau below $T \approx 50$ K (Figure 3C), thus supporting the model discussed above. The slow processes of SLR can directly be related to ZFS values of less than 1 cm^{-1}.[1,2,56−59] A correspondingly small value is only possible if SOC-induced mixing of higher-lying singlet or triplet MLCT states with the lowest triplet substates is very weak. This result corresponds perfectly to the predictions based on the very simple considerations given in section 2.1. Furthermore, the emission decay time of the triplet state T_1 of $\tau(T_1)$ = 1200 μs, as found in the range of the plateau below $T \approx 50$ K (Figure 3C), is extremely long compared to other copper(I) complexes (see below and refs 5, 7−10, 13−16, 19−24, and 34), and again this is a consequence of the weak SOC with respect to this state. With a temperature increase, the decay time decreases drastically to τ(300 K) = 3.3 μs. Accordingly, the radiative rate k^r, determined by using $k^r = \phi_{PL}/\tau$, rises from the low-temperature value of k^r(30 K) = 8.3 × 10^2 s^{-1} to k^r(300 K) = 2.1 × 10^5 s^{-1}, being a rate increase of more than a factor of 250 (compare Table 1).

This drastic radiative rate increase combined with the observed blue shift with a temperature increase from $T \approx 30$ to 300 K can only be explained by an involvement of a higher-lying energy state that carries a high radiative rate, hence demonstrating the occurrence of TADF. As depicted in Figure 3D, at low temperature only long-lived phosphorescence from the T_1 state to the singlet ground state S_0 is observed. With growing temperature from above $T \approx 50$ K, a fast up-ISC to the S_1 state takes place in a time range of several pico-seconds[45,46,61−63] and opens the additional radiative process as TADF via the singlet state S_1. This process induces the drastic increase of the radiative rate and leads to a blue shift of the emission because the S_1 state lies at higher energy than the T_1 state.

Because of the fast thermal equilibration between the T_1 and S_1 states, i.e., the fast up- and down-ISC processes (above $T \approx 20$ K), the emission decay time τ can be expressed by a Boltzmann-type equation:[1,2,5,7−10,14,54]

$$\tau(T) = \frac{3 + \exp[-\Delta E(S_1 - T_1)/k_B T]}{3/\tau(T_1) + 1/\tau(S_1)\exp[-\Delta E(S_1 - T_1)/k_B T]} \quad (1)$$

wherein k_B denotes the Boltzmann constant. $\tau(T_1)$ and $\tau(S_1)$ represent the phosphorescence ($T_1 \rightarrow S_0$) and prompt fluorescence ($T_1 \rightarrow S_0$) decay times without thermal activation. $\Delta E(S_1{-}T_1)$ is the energy separation between these two states.

Applying this relationship to the measured emission decay times (Figure 3B,C) and using the value of $\tau(T_1)$ = 1.2 ms as measured directly for T < 50 K, one obtains the fit parameters for the activation energy of $\Delta E(S_1{-}T_1)$ = 370 cm^{-1} and for the prompt fluorescence decay time of $\tau(S_1)$ = 180 ns. It is remarked that the prompt fluorescence could not be observed directly according to the very fast down-ISC processes of only a

Table 1. Emission Data for Powder Samples of Different Copper(I) Complexes Showing TADF

	300 K				80 K				30 K			fit		
compound	λ_{max} [nm]	ϕ_{PL} [%]	τ [μs]	k^r [s^{-1}]	λ_{max} [nm]	ϕ_{PL} [%]	τ [μs]	k^r [s^{-1}]	λ_{max} [nm]	τ [μs]	k^r[a] [s^{-1}]	$\tau(S_1)$ [ns]	$\Delta E(S_1{-}T_1)$ [cm^{-1}]	ref
Cu(dppb)(pz$_2$Bph$_2$) (**1**)	535	70	3.3	21 × 10^4	535	≈100	300	3.3 × 10^3	548	1200	0.83 × 10^3	180	370	this work
Cu(pop)(pz$_2$Bph$_2$) (**2**)	464	90	13	6.9 × 10^4	474	≈100	500	2.0 × 10^3	474	500	2.0 × 10^3	170	650	2, 9
Cu(dmp)(phanephos)$^+$ (**3**)	530	80	14	5.7 × 10^4	562	70	240	2.9 × 10^3	562	240	2.9 × 10^3	40	1000	10

[a]It is assumed that the values of ϕ_{PL} at T = 30 K amount to 100%, as determined experimentally at T = 80 K.

DOI: 10.1021/ic503072u
Inorg. Chem. 2015, 54, 4322−4327

few picoseconds.[45,46,61−63] The resulting energy level diagram and relevant decay processes are summarized in Figure 3D.

Indeed, the experimental characterization of the luminescence behavior of compound **1** fits well to the predictions developed in section 2.1. According to the distinct spatial separation of the HOMO and LUMO frontier orbitals involved in the lowest excited states, the fluorescence decay time of $\tau(S_1)$ = 180 ns is relatively long for a spin-allowed transition. Moreover, as expected, the energy separation between the lowest singlet and triplet excited states is very small. The value of $\Delta E(S_1-T_1)$ = 370 cm^{-1} represents the smallest splitting value found so far. Accordingly, compound **1** shows the shortest TADF decay time, τ(TADF) = 3.3 μs, that has been reported for copper(I) complexes until now. Similarly, the very weak efficiency of SOC, as concluded from simple considerations of energy separations between the relevant frontier orbitals, could be verified experimentally. For completeness, it is remarked that a $\Delta E(S_1-T_1)$ value of 167 cm^{-1} was previously reported for this complex blended in 1,3-bis(*N*-carbazolyl)benzene. The value was determined from a comparison of the emission maxima measured at 77 and 300 K, respectively[18] However, taking into account the very small singlet−triplet splitting and the occurrence of a strong TADF component even at 77 K with an emission maximum at almost the same energy as that found at ambient temperature, this value is strongly underestimated (compare also the next section).

2.3. Wide Range of TADF Properties of Different Copper(I) Complexes. Analogous studies performed for compounds **2** and **3** (Figure 4 and Table 1) reveal that the

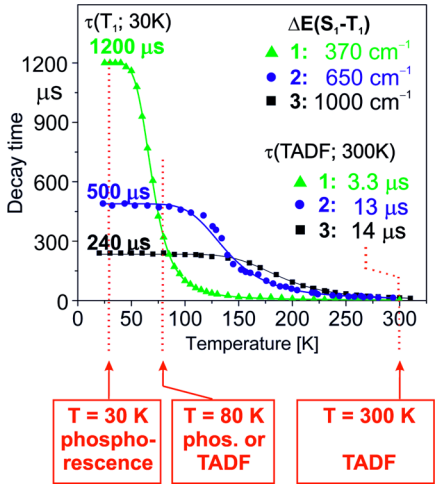

Figure 4. Luminescence decay times of **1** (green triangles), **2** (blue circles), and **3** (black squares) versus temperature for powder samples. The dominant emission mechanisms at 30, 80, and 300 K are indicated.

emission at ambient temperature is also clearly of TADF character though with distinctly larger energy separations $\Delta E(S_1-T_1)$ of 650 cm^{-1} (**2**) and 1000 cm^{-1} (**3**) compared to the value of only 370 cm^{-1} for compound **1** (Table 1). Accordingly, with a temperature decrease, TADF is frozen out at already relatively high temperatures. Thus, the phosphorescence plateau of compounds **3** and **2** is reached at $T \approx 150$ and 100 K, respectively, while for compound **1**, cooling to below $T \approx 50$ K is required. As a consequence, the emission of compounds **2** and **3** at T = 80 K can clearly be classified as phosphorescence stemming from the T_1 state, while the emission of compound **1** with a decay time of τ(80 K) = 300 μs cannot be assigned as phosphorescence but represents mainly delayed fluorescence (TADF). By use of the equations given in ref 8, the ratio of fluorescence to phosphorescence intensity can be estimated at 3 to 1. Hence, assignments with respect to the emission characteristics as phosphorescence or fluorescence (TADF) might be problematic for copper(I) compounds if investigations can only be carried out at 300 and 80 K, as was frequently reported. Similar arguments hold also for the assignments of the spectral shifts between phosphorescence and TADF (Figure 3A).

Table 1 summarizes the photophysical data of the three compounds. The most important differences are dictated by the energy separation $\Delta E(S_1-T_1)$, which, in turn, is mainly given by the spatial separation between HOMO and LUMO (section 2.1 and the SI). The very small value of $\Delta E(S_1-T_1$, **1**) = 370 cm^{-1} is responsible for the relatively high radiative rate at T = 300 K of k^r(300 K, **1**) = 2.1 × 10^5 s^{-1} being only by a factor of about 3 smaller than the radiative rate found for the well-known $Ir(ppy)_3$ complex (with ppy = 2-phenylpyridine).[1,2,64] Moreover, because of the largely forbidden nature of the $T_1 \rightarrow S_0$ transition with a radiative rate of only k^r(30 K, **1**) = 8.3 × 10^2 s^{-1}, the TADF effect induces a rate increase by more than a factor of 250 with a temperature increase from T = 30 to 300 K. The effect is much less pronounced for **2** and **3** with rate increases of about 35 and 20 times, respectively. Obviously, compound **1** of this series showing the smallest $\Delta E(S_1-T_1)$ value can attain the highest TADF transition rate at ambient temperature, although the decay time of its triplet state is by far the longest one (smallest radiative decay rate).

The radiative rates of the triplet T_1 states vary in this series from 8.3 × 10^2 s^{-1} (**1**) to 2.0 × 10^3 s^{-1} (**2**) to 2.9 × 10^3 s^{-1} (**3**). This tells us that the SOC efficiency increases distinctly, which is related to the energy separation between HOMO−1 and HOMO. This trend is well displayed by TD-DFT approaches. Because the lowest triplet state T_1 being of ^{3}MLCT character is largely of HOMO → LUMO origin, singlet states of HOMO−1 → LUMO character that may induce oscillator strengths by SOC because of the contribution of different d orbitals[1,2,S1,S2] are the states S_6 for compound **1**, S_2 for **2**, and S_3 for **3** with energy separations of 1.54, 0.79, and 0.87 eV, respectively (Tables S1−S3 in the SI). For completeness, it is remarked that apparently the corresponding energy separations are still too large to induce ZFS of more than 1 or 2 cm^{-1}, in contrast to the situation observed for $Cu_2Cl_2(N^P)_2$.[23]

The decay times of the prompt $S_1 \rightarrow S_0$ fluorescence, as determined by fitting procedures, amount to $\tau(S_1)$ = 180 ns (**1**), 170 ns (**2**), and 40 ns (**3**), respectively. Corresponding calculated oscillator strengths resulting from TD-DFT approaches display a similar trend (Tables S1−S3 in the SI). These values show an opposite trend compared to the energy separations $\Delta E(S_1-T_1)$ (Table 1). As discussed above, both trends are related to the spatial overlap of HOMO and LUMO. For completeness, it is remarked that for compound **3** it has been shown that the radiative rate of $k^r(S_1 \rightarrow S_0)$ = 2 × 10^7 s^{-1} fits well to the related value as determined from the absorption spectrum by use of the Strickler−Berg relation.[10]

3. CONCLUSIONS

The tetracoordinated copper(I) complexes studied in this contribution represent a class of brightly emitting luminescent materials with no concentration quenching and high emission

DOI: 10.1021/ic503072u
Inorg. Chem. 2015, 54, 4322−4327

quantum yields of $\phi_{PL} \geq 70\%$. The pronounced charge-transfer character of the emitting states is associated with a relatively small quantum-mechanical exchange interaction, thus giving small energy separations $\Delta E(S_1-T_1)$ between the lowest singlet S_1 (^{1}MLCT) and triplet T_1 (^{3}MLCT) states. As a consequence, the higher-lying singlet state can be populated significantly at ambient temperature, resulting in TADF. According to this property, the (radiative) TADF decay time is much shorter than the compound's phosphorescence decay time. Thus, such complexes have become highly attractive for applications as OLED emitters because, making use of the TADF effect, all singlet and triplet excitons can be exploited and harvested in the singlet state, representing the singlet-harvesting mechanism.

The compounds discussed in this contribution exhibit energy separations $\Delta E(S_1-T_1)$ over the extensive range of 370−1000 cm^{-1}. Accordingly, very different emission properties are observed. These differences are particularly well-displayed in the temperature dependence of the emission decay if studied over a very large temperature range, that is at least from ambient temperature down to $T \approx 30$ K or even lower. Especially, it is shown that the energy separation $\Delta E(S_1-T_1)$, dominating the material's photophysical properties, should be as small as possible. Interestingly, **1** exhibits the smallest value of $\Delta E(S_1-T_1) = 370$ cm^{-1} reported so far. As a consequence, a very short emission decay time at ambient temperature of only τ(TADF) = 3.3 μs (corresponding to a radiative decay time of τ^r(TADF) = 4.7 μs) results, although the phosphorescence decay time of the $T_1 \rightarrow S_0$ transition is as long as 1.2 ms. A short decay time is highly advantageous if the compound is applied as an emitter in an OLED because saturation or roll-off effects are less important compared to long-lived emitters.[43] In this respect, the TADF compound **1** may be compared to one of the most efficient organic TADF molecules. For example, Adachi et al. proposed the use of (4*S*,6*S*)-2,4,5,6-tetra(9*H*-carbazol-9-yl)isophthalonitrile. This emitter shows an ambient temperature decay time of τ(TADF) = 5.1 μs at a ϕ_{PL} value of 94%,[33] giving a radiative decay time of τ^r(TADF) = τ(TADF)/ϕ_{PL} = 5.4 μs. Hence, if focused on short (radiative) TADF decay times, it can be concluded that copper(I) complexes showing TADF may be well comparable or even slightly better than purely organic TADF molecules.

■ ASSOCIATED CONTENT

Supporting Information

Experimental details of the photophysical measurements and quantum chemical computations. This material is available free of charge via the Internet at http://pubs.acs.org.

■ AUTHOR INFORMATION

Corresponding Authors

*E-mail: rafal.czerwieniec@ur.de.
*E-mail: hartmut.yersin@ur.de.

Notes

The authors declare no competing financial interest.

■ ACKNOWLEDGMENTS

The authors gratefully acknowledge the German Ministry of Education and Research (BMBF) for funding.

■ REFERENCES

(1) Yersin, H.; Rausch, A. F.; Czerwieniec, R.; Hofbeck, T.; Fischer, T. *Coord. Chem. Rev.* **2011**, *255*, 2622−2652.
(2) Yersin, H.; Rausch, A. F.; Czerwieniec, R. In *Physics of Organic Semiconductors*; Brütting, W., Adachi, C. Eds.; Wiley-VCH: Weinheim, Germany, 2012; p 371.
(3) Breddels, P.; Berdowski, P. A. M.; Blasse, G.; McMillin, D. R. *J. Chem. Soc., Faraday Trans. 2* **1982**, *78*, 595−601.
(4) Felder, D.; Nierengarten, J.-F.; Barigelletti, F.; Ventura, B.; Armaroli, N. *J. Am. Chem. Soc.* **2001**, *123*, 6291−6299.
(5) Leitl, M. J.; Krylova, V. A.; Djurovich, P. I.; Thompson, M. E.; Yersin, H. *J. Am. Chem. Soc.* **2014**, *136*, 16032−16038.
(6) Abedin-Siddique, Z.; Ohno, T.; Nozaki, K. *Inorg. Chem.* **2004**, *43*, 663−673.
(7) Linfoot, C. L.; Leitl, M. J.; Richardson, P.; Rausch, A. F.; Chepelin, O.; White, F. J.; Yersin, H.; Robertson, N. *Inorg. Chem.* **2014**, *53*, 10854−10861.
(8) Leitl, M. J.; Küchle, F.-R.; Mayer, H. A.; Wesemann, L.; Yersin, H. *J. Phys. Chem. A* **2013**, *117*, 11823−11836.
(9) Czerwieniec, R.; Yu, J.; Yersin, H. *Inorg. Chem.* **2011**, *50*, 8293−8301.
(10) Czerwieniec, R.; Kowalski, K.; Yersin, H. *Dalton Trans.* **2013**, *42*, 9826−9830.
(11) Armaroli, N. *Chem. Soc. Rev.* **2001**, *30*, 113−124.
(12) Endo, A.; Ogasawara, M.; Takahashi, A.; Yokoyama, D.; Kato, Y.; Adachi, C. *Adv. Mater.* **2009**, *21*, 4802−4806.
(13) Tsuboyama, A.; Kuge, K.; Furugori, M.; Okada, S.; Hoshino, M.; Ueno, K. *Inorg. Chem.* **2007**, *46*, 1992−2001.
(14) Deaton, J. C.; Switalski, S. C.; Kondakov, D. Y.; Young, R. H.; Pawlik, T. D.; Giesen, D. J.; Harkins, S. B.; Miller, A. J. M.; Mickenberg, S. F.; Peters, J. C. *J. Am. Chem. Soc.* **2010**, *132*, 9499−9508.
(15) (a) Wallesch, M.; Volz, D.; Fléchon, C.; Zink, D. M.; Bräse, S.; Baumann, T. *Proc. SPIE* **2014**, *9183*, 918309−1. (b) Volz, D.; Chen, Y.; Wallesch, M.; Liu, R.; Fléchon, C.; Zink, D. M.; Friedrichs, J.; Flügge, H.; Steininger, R.; Göttlicher, J.; Heske, C.; Weinhardt, L.; Bräse, S.; So, F.; Baumann, T. *Adv. Mater.* **2015**, *27*, 2538−2543.
(16) Wallesch, M.; Volz, D.; Zink, D. M.; Schepers, U.; Nieger, M.; Baumann, T.; Bräse, S. *Chem.—Eur. J.* **2014**, *20*, 6578−6590.
(17) Zink, D. M.; Volz, D.; Baumann, T.; Mydlak, M.; Flügge, H.; Friedrichs, J.; Nieger, M.; Bräse, S. *Chem. Mater.* **2013**, *25*, 4471−4486.
(18) Igawa, S.; Hashimoto, M.; Kawata, I.; Yashima, M.; Hoshino, M.; Osawa, M. *J. Mater. Chem. C* **2013**, *1*, 542−551.
(19) Bizzarri, C.; Strabler, C.; Prock, J.; Trettenbrein, B.; Ruggenthaler, M.; Yang, C.-H.; Polo, F.; Iordache, A.; Brüggeller, P.; De Cola, L. *Inorg. Chem.* **2014**, *53*, 10944−10951.
(20) Osawa, M.; Hoshino, M.; Hashimoto, M.; Kawata, I.; Igawa, S.; Yashima, M. *Dalton Trans.* DOI: 10.1039/C4DT02853H.
(21) Gneuß, T.; Leitl, M. J.; Finger, L. H.; Rau, N.; Yersin, H.; Sundermeyer, J. *Dalton Trans.* DOI: 10.1039/c4dt02631d.
(22) Ohara, H.; Kobayashi, A.; Kato, M. *Dalton Trans.* **2014**, *43*, 17317−17323.
(23) Hofbeck, T.; Monkowius, U.; Yersin, H. *J. Am. Chem. Soc.* **2015**, *137*, 399−404.
(24) Chen, X.-L.; Yu, R.; Zhang, Q.-K.; Zhou, L.-J.; Wu, X.-Y.; Zhang, Q.; Lu, C.-Z. *Chem. Mater.* **2013**, *25*, 3910−3920.
(25) Zink, D. M.; Bächle, M.; Baumann, T.; Nieger, M.; Kuhn, M.; Wang, C.; Klopper, W.; Monkowius, U.; Hofbeck, T.; Yersin, H.; Bräse, S. *Inorg. Chem.* **2013**, *52*, 2292−2305.
(26) Penzkofer, A.; Tyagi, A.; Slyusareva, E.; Sizykh, A. *Chem. Phys.* **2010**, *378*, 58−65.
(27) Baleizão, C.; Berberan-Santos, M. N. *Ann. N.Y. Acad. Sci.* **2008**, *1130*, 224−234.
(28) Endo, A.; Sato, K.; Yoshimura, K.; Kai, T.; Kawada, A.; Miyazaki, H.; Adachi, C. *Appl. Phys. Lett.* **2011**, *98*, 083302.
(29) Zhang, Q.; Li, B.; Huang, S.; Nomura, H.; Tanaka, H.; Adachi, C. *Nat. Photonics* **2014**, *8*, 326−332.
(30) Tanaka, H.; Shizu, K.; Nakanotani, H.; Adachi, C. *J. Phys. Chem. C* **2014**, *118*, 15985−15994.

DOI: 10.1021/ic503072u
Inorg. Chem. 2015, 54, 4322−4327

(31) Cho, Y. J.; Yook, K. S.; Lee, J. Y. *Adv. Mater.* **2014**, *26*, 6642−6646.
(32) Jones, P. F.; Calloway, A. R. *Chem. Phys. Lett.* **1971**, *10*, 438−443.
(33) Uoyama, H.; Goushi, K.; Shizu, K.; Nomura, H.; Adachi, C. *Nature* **2012**, *492*, 234−238.
(34) Xiong, X.; Song, F.; Wang, J.; Zhang, Y.; Xue, Y.; Sun, L.; Jiang, N.; Gao, P.; Tian, L.; Peng, X. *J. Am. Chem. Soc.* **2014**, *136*, 9590−9597.
(35) Tao, Y.; Yuan, K.; Chen, T.; Xu, P.; Li, H.; Chen, R.; Zheng, C.; Zhang, L.; Huang, W. *Adv. Mater.* **2014**, *26*, 7931−7958.
(36) Wei, F.; Qiu, J.; Liu, X.; Wang, J.; Wei, H.; Wang, Z.; Liu, Z.; Bian, Z.; Lu, Z.; Zhao, Y.; Huang, C. *J. Mater. Chem. C* **2014**, *2*, 6333−6341.
(37) Liu, Z.; Qiu, J.; Wei, F.; Wang, J.; Liu, X.; Helander, M. G.; Rodney, S.; Wang, Z.; Bian, Z.; Lu, Z.; Thompson, M. E.; Huang, C. *Chem. Mater.* **2014**, *26*, 2368−2373.
(38) Keller, S.; Constable, E. C.; Housecroft, C. E.; Neuburger, M.; Prescimone, A.; Longo, G.; Pertegás, A.; Sessolo, M.; Bolink, H. J. *Dalton Trans.* **2014**, *43*, 16593−16596.
(39) Armaroli, N.; Accorsi, G.; Holler, M.; Moudam, O.; Nierengarten, J.-F.; Zhou, Z.; Wegh, R. T.; Welter, R. *Adv. Mater.* **2006**, *18*, 1313−1316.
(40) Costa, R. D.; Tordera, D.; Ortí, E.; Bolink, H. J.; Schönle, J.; Graber, S.; Housecroft, C. E.; Constable, E. C.; Zampese, J. A. *J. Mater. Chem.* **2011**, *21*, 16108−16118.
(41) Yersin, H., Ed. *Highly Efficient OLEDs with Phosphorescent Materials*; Wiley-VCH: Berlin, 2008.
(42) Adachi, C.; Baldo, M. A.; Thompson, M. E.; Forrest, S. R. *J. Appl. Phys.* **2001**, *90*, 5048−5051.
(43) Murawski, C.; Leo, K.; Gather, M. C. *Adv. Mater.* **2013**, *25*, 6801−6827.
(44) Atkins, P. W. *Quanta. A Handbook of Concepts*, 2nd ed.; Oxford University Press: Oxford, U.K., 1991.
(45) Iwamura, M.; Watanabe, H.; Ishii, K.; Takeuchi, S.; Tahara, T. *J. Am. Chem. Soc.* **2011**, *133*, 7728−7736.
(46) Shaw, G. B.; Grant, C. D.; Shirota, H.; Castner, E. W., Jr.; Meyer, G. J.; Chen, L. X. *J. Am. Chem. Soc.* **2007**, *129*, 2147−2160.
(47) Lavie-Cambot, A.; Cantuel, M.; Leydet, M.; Jonusauskas, G.; Bassani, D. M.; McClenaghan, N. D. *Coord. Chem. Rev.* **2008**, *252*, 2572−2584.
(48) Vorontsov, I. I.; Graber, T.; Kovalevsky, A. Y.; Novozhilova, I. V.; Gembicky, M.; Chen, Y.-S.; Coppens, P. *J. Am. Chem. Soc.* **2009**, *131*, 6566−6573.
(49) Rausch, A. F.; Homeier, H. H. H.; Yersin, H. *Top. Organomet. Chem.* **2010**, 193−235.
(50) El-Sayed, M. A. *J. Chem. Phys.* **1963**, *38*, 2834−2838.
(51) Kimachi, S.; Satomi, R.; Miki, H.; Maeda, K.; Azumi, T. *J. Phys. Chem. A* **1997**, *101*, 345−349.
(52) Yersin, H.; Monkowius, U.; Czerwieniec, R.; Yu, J. Patents WO002010031485AI, DE102008336AI, 2008.
(53) Photoinduced molecular geometry changes in the MLCT excited states, although largely suppressed in the relatively rigid environment of a powder sample, induce a self-trapping of the excitation, which results in its localization.[1,9] This allows us to investigate solid samples because energy transfer to neighboring emitter molecules and concentration quenching are not important.
(54) Yersin, H.; Leitl, M. J.; Czerwieniec, R. *Proc. SPIE* **2014**, *9183*, 91830N.
(55) Yersin, H.; Strasser, J. *Coord. Chem. Rev.* **2000**, *208*, 331−364.
(56) Yersin, H.; Donges, D. *Top. Curr. Chem.* **2001**, *214*, 81−186.
(57) Schmidt, J.; Wiedenhofer, H.; von Zelewsky, J.; Yersin, H. *J. Phys. Chem.* **1995**, *99*, 226−229.
(58) Czerwieniec, R.; Finkenzeller, W. J.; Hofbeck, T.; Starukhin, A.; Wedel, A.; Yersin, H. *Chem. Phys. Lett.* **2009**, *468*, 205−210.
(59) Prokhorov, A. M.; Hofbeck, T.; Czerwieniec, R.; Suleymanova, A. F.; Kozhevnikov, D. N.; Yersin, H. *J. Am. Chem. Soc.* **2014**, *136*, 9637−9642.
(60) Tinti, D. S.; El-Sayed, M. A. *J. Chem. Phys.* **1971**, *54*, 2529−2549.
(61) Hua, L.; Iwamura, M.; Takeuchi, S.; Tahara, T. *Phys. Chem. Chem. Phys.* **2015**, *17*, 2067−2077.
(62) Papanikolaou, P. A.; Tkachenko, N. V. *Phys. Chem. Chem. Phys.* **2013**, *15*, 13128−13136.
(63) Tschierlei, S.; Karnahl, M.; Rockstroh, N.; Junge, H.; Beller, M.; Lochbrunner, S. *Chem. Phys. Phys. Chem.* **2014**, *15*, 3709−3713.
(64) Hofbeck, T.; Yersin, H. *Inorg. Chem.* **2010**, *49*, 9290−9299.

DOI: 10.1021/ic503072u
Inorg. Chem. 2015, 54, 4322−4327